学　位　論　文

Role of Mir-452-5p Overexpression in Epithelial–Mesenchymal Transition (EMT) in Early-stage Colorectal Cancer

香川大学大学院医学系研究科

医学専攻

小山　裕紀子

in vivo *37*: 1980-1990 (2023)
doi:10.21873/invivo.13295

Role of Mir-452-5p Overexpression in Epithelial–Mesenchymal Transition (EMT) in Early-stage Colorectal Cancer

YUKIKO KOYAMA[1], SHINTARO FUJIHARA[1], TAIGA CHIYO[1], TAKANORI MATSUI[1], SAE HAMAYA[1], KOJI FUJITA[1], JOJI TANI[1], ASAHIRO MORISHITA[1], HIDEKI KOBARA[1], MASAFUMI ONO[1], HISAKAZU IWAMA[2] and TSUTOMU MASAKI[1]

[1]*Department of Gastroenterology and Neurology, Faculty of Medicine, Kagawa University, Kagawa, Japan;*
[2]*Life Science Research Center, Kagawa University, Kagawa, Japan*

Abstract. *Background/Aim: The microRNA miR-452-5p holds a critical role in the progression of multiple tumor formations, but there is limited understanding regarding the epithelial-mesenchymal transition (EMT) progression and its underlying mechanisms in the early-stage colorectal cancer (CRC). We aimed to explore the change in miRNA expression in early-stage CRC and examine the role of these miRNAs in CRC. Materials and Methods: The expression levels of miR-452-5p in tissues and cells of early-stage CRC were determined by real-time quantitative polymerase chain reaction. Additionally, the biological effects of miR-452-5p on CRC were investigated by in vitro functional experiments. Results: The expression levels of miR-452-5p were found increased in early-stage CRC tissue. We found that miR-452-5p promoted CRC cell proliferation but inhibited epithelial–mesenchymal transition. Furthermore, miR-452-5p promoted cell proliferation through activation of the extracellular signal-regulated kinase pathway, and inhibited cell invasion through suppression of Slug (Snail2) expression and up-regulation of E-cadherin expression. Conclusion: The expression of miR-452-5p is up-regulated in early CRC and suppresses epithelial–mesenchymal transition in CRC. These discoveries suggest that miR-452-5p has the potential to serve as a viable therapeutic target for CRC.*

Correspondence to: Yukiko Koyama, MD, Department of Gastroenterology and Neurology, Kagawa University Faculty of Medicine, Graduate School of Medicine,1750-1 Ikenobe, Miki-cho, Kita-gun, Kagawa 761-0793, Japan. Tel: +81 878912156, Fax: +81 878912158, e-mail: koyama.yukiko@kagawa-u.ac.jp

Key Words: Colorectal cancer, miR-452-5p, epithelial–mesenchymal transition.

Colorectal cancer (CRC) is the third most common cancer worldwide and the leading cause of cancer-related death (1). In recent years, screening colonoscopy has achieved great success in the early detection of CRC, but most patients are diagnosed at an advanced stage and have a poor prognosis. Metastasis is closely associated with epithelial–mesenchymal transition (EMT) in which cells gradually lose their epithelial phenotype and acquire a mesenchymal phenotype (2). EMT is one of the main steps in the progression of tumors. Numerous studies have shown that EMT is necessary for the increased invasive potential of tumour cells in progression of various types of cancer (3). Cancer cells undergoing EMT show reduced expression of epithelial markers, such as E-cadherin and β-catenin, and increased expression of mesenchymal markers, such as N-cadherin and vimentin (4). Therefore, more intensive research on the molecular mechanisms of early-stage CRC is urgently required to identify early diagnostic markers and potential therapeutic targets.

The regulation of E-cadherin plays an important role in tumor progression, and several growth factors (transforming growth factor, hepatocyte growth factor, and epidermal growth factor) and transcriptional inhibitors (Snail, Slug, Twist, and ZEB1/2) are involved in the regulation of EMT (5). Snail is a transcriptional inhibitor of the E-cadherin Snail protein family, and it includes Snail1, Snail2 (Slug), and Snail3 (Smuc). Snail proteins bind specifically to the E-box element of the E-cadherin gene *via* the zinc finger domain (6). Slug is highly expressed in patients with CRC and promotes CRC cell invasion (7). Additionally, Slug may epigenetically suppress E-cadherin expression in CRC metastasis.

MicroRNAs (miRNAs) are a type of short, single-stranded, non-coding RNAs that interact with mRNA through pairing of complementary sequences in the 3' untranslated region of target genes, resulting in mRNA degradation and translation failure (8). The miRNA miR-452-5p is a regulator of colorectal, liver, and lung cancer, specifically promoting cancer cell invasion, migration, and proliferation (9). More importantly, miR-452-5p is abnormally expressed in CRC (9).

Table I. *Patient characteristics.*

Case	Sample No.	Sex	Age	Location	Tumor size (mm)	Clinical diagnosis	Definitive diagnosis	Lymphovascular invasion
1	1	M	74	T	30×18	M	Adenoma	(-)
2	2	M	84	A	17×11	M	SM2	(V+)
3	7	F	81	T	17×15	Adenoma	Adenoma	(-)
4	8	M	87	A	27×24	SM	M	(-)
5	9	M	91	Ra	65×45	M	M	(-)
6	10	F	89	Ra	60×40	M	SM1	(-)
7	11	M	61	S	17×17	M	Adenoma	(-)
8	12	M	88	Rb	26×20	M	SM1	(-)
9	13	F	69	A	25×20	M	Adenoma	(-)
10	14	F	75	S	30×17	M	SM2	(Ly+)
11	15	F	74	C	12×7	SM	SM2	(V+)
12	16	M	68	T	25×20	SM2	SM2	(V+)
13	18	M	59	A	10×8	SM2	SM2	(Ly+, V+)
14	19	F	95	Rb	38×22	SM2	SM2	(V+)
15	20	M	57	Ra	15×10	SM2	SM2	(Ly+, V+)

M: Male; F: female; T: transverse colon; A: ascending colon; C: cecum; S: sigmoid colon; Ra: rectum (above the peritoneal reflection); Rb: rectum (below the peritoneal reflection); M: mucosal; SM1: submucosal invasion <1,000 μm; SM2: submucosal invasion ≥1,000 μm; Ly: lymphatic invasion; V: venous invasion.

The expression level of miR-452-5p is significantly down-regulated in advanced CRC tissues, promoting invasion and metastasis, which are associated with a poor clinical prognosis (10). In contrast, there is a report that miR-452-5p is overexpressed in advanced CRC and it promotes cell proliferation, cell cycle transition, and chemotherapy resistance and inhibits cell apoptosis. However, EMT of miR-452-5p in early-stage CRC and its mechanisms have not been fully clarified.

In this study, we investigated the involvement of miR-452-5p in cell proliferation and invasion in CRC. To investigate cell invasion, we focused on EMT.

Materials and Methods

Patients and samples. Early CRC tissue and adjacent normal tissue were collected from 20 patients who underwent colonoscopic endoscopic submucosal dissection (ESD) at the Kagawa University Hospital from April 2017 to March 2018. The patient underwent tumor resection by ESD after a clinical and pathologic diagnosis of stage I CRC. Colorectal neoplasms were histologically classified as serrated lesions, adenomas, intramucosal carcinomas, SM1 carcinomas with superficial (<1,000 μm) submucosal invasion, and SM2 carcinoma with deep (≥1,000 μm) submucosal invasion. Intramucosal carcinomas were defined as mucosal high-grade neoplasia (category 4) and submucosal carcinomas represented invasive carcinoma (category 5) in the revised Vienna Classification (11).

All patients underwent ESD according to a standardized protocol without any treatment for their tumor before ESD. Biopsy samples of the tumor and adjacent normal tissue were taken from each patient immediately before completing ESD. The sampling procedure was the same as that described in our previous study (12). All tissue samples were frozen immediately after excision and

Table II. *Summary of significantly up-regulated and down-regulated miRNAs between early CRC and adjacent normal tissue.*

miRNA	Fold change (Tumor/Normal)	*p*-Value	FDR
Up-regulated			
has-miR-4633-5p	2,401734	0,000025	0,001198
has-miR-452-5p	2,312177	0,000377	0,010005
has-miR-3907	2,266059	0,000032	0,001440
has-miR-4299	1,929717	0,000055	0,002172
hsa-miR-4730	1,928920	0,000017	0,001033
has-miR-887-5p	1,876268	0,000457	0,011287
has-miR-8059	1,790614	0,000006	0,001033
has-miR-1285-3p	1,673807	0,000218	0,006789
has-miR-769-5p	1,634738	0,000076	0,002877
has-miR-6876-5p	1,567126	0,000018	0,001033
has-miR-3663-3p	1,525760	0,000372	0,010005
Down-regulated			
hsa-miR-133b	0,324593	0,000013	0,001033
hsa-miR-133a-3p	0,380456	0,000151	0,004900
hsa-miR-378g	0,444162	0,000005	0,001033
hsa-miR-378c	0,452104	0,000016	0,001033
hsa-miR-378d	0,454092	0,000019	0,001033
hsa-miR-378e	0,464034	0,000015	0,001033
hsa-miR-378f	0,467831	0,000009	0,001033
hsa-miR-378b	0,469599	0,000001	0,000433
hsa-miR-378i	0,470580	0,000012	0,001033
hsa-miR-572	0,479847	0,000412	0,010528
hsa-miR-378a-5p	0,516377	0,000044	0,001854
hsa-miR-3185	0,555634	0,000279	0,008322
hsa-miR-378a-3p	0,558695	0,000002	0,000677
hsa-miR-638	0,610290	0,000324	0,009267
hsa-miR-4731-5p	0,647158	0,000019	0,001033

Fold change (FC)>1.5 and FC<0.67, $p<0.001$. CRC: Colorectal cancer; FDR: false discovery rate.

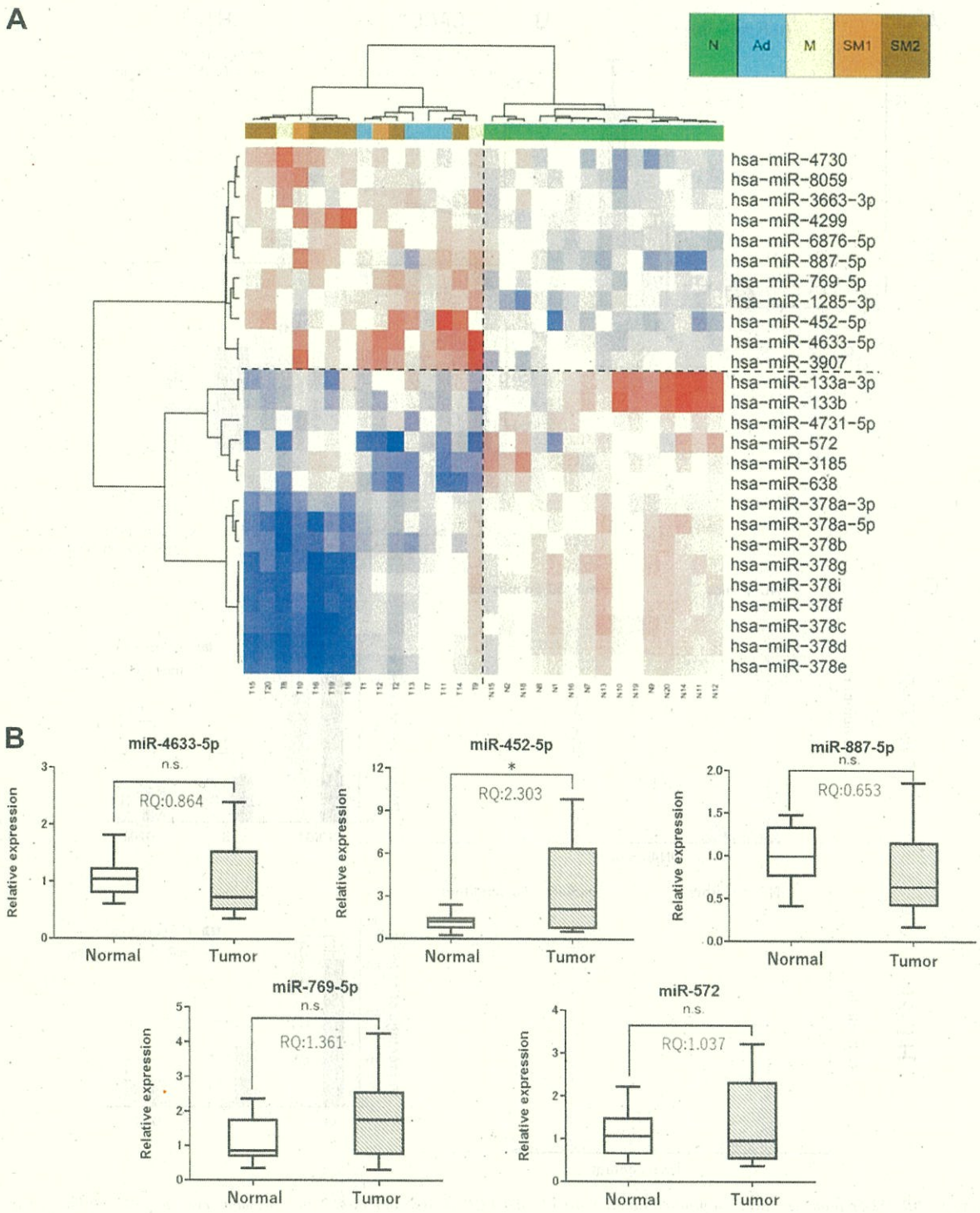

Figure 1. *Differences in miRNA expression between early-stage CRC and adjacent normal tissue. (A) Hierarchical clustering of expression profiles of numerous differentially expressed miRNA between early-stage CRC and adjacent normal tissue. The columns represent the patients, and the rows represent the individual miRNAs. Red indicates a high expression level and blue indicates a low expression level. (B) qRT-PCR analysis of miR-4633-5p, miR-452-5p, miR-887-5p, miR-769-5p, and miR-572 in 15 paired samples of CRC tissue compared with adjacent normal tissue. The* $2^{-\Delta\Delta CT}$ *method was used to analyze relative quantification of miRNAs. Data represent the mean±standard deviation. *p<0.05 vs. the control group. CRC: Colorectal cancer; qRT-PCR: real-time quantitative reverse transcription-polymerase chain reaction; RQ: relative quantity.*

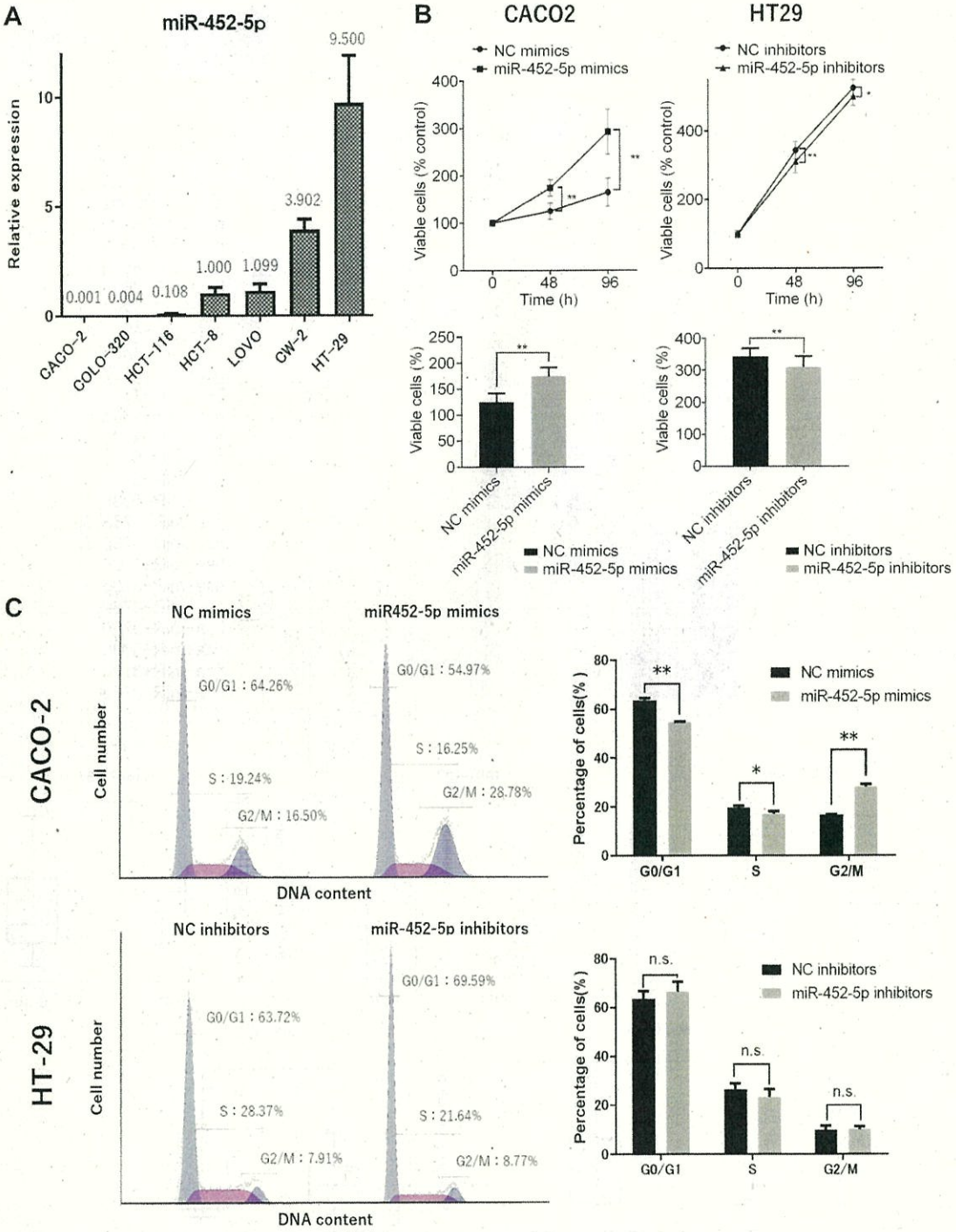

Figure 2. *MiR-452-5p promotes CRC cell proliferation in vitro. (A) qRT-PCR analysis of miR-452-5p expression levels in CRC cell lines compared to HCT8 as the standard. (B) CACO-2 cells were transfected with control RNAs or miR-452-5p mimics, and HT-29 cells were transfected with control RNAs or miR-452-5p inhibitors. The viability of cells was evaluated using the CCK-8 assay. Upper panels: cell viability was assayed at 0, 48, and 96 h. Lower panels: cell viability of these cells at 48 h. (C) Left panels: effect of overexpression and repression of miR-452-5p on the CRC cell cycle. The results were analyzed by flow cytometry. Right panels: graphical representation of the proportion of cells in each phase of the cell cycle. Data represent the mean±standard deviation. *p<0.05, **p<0.01 vs. the control group. CRC: Colorectal cancer; qRT-PCR: real-time quantitative reverse transcription-polymerase chain reaction.*

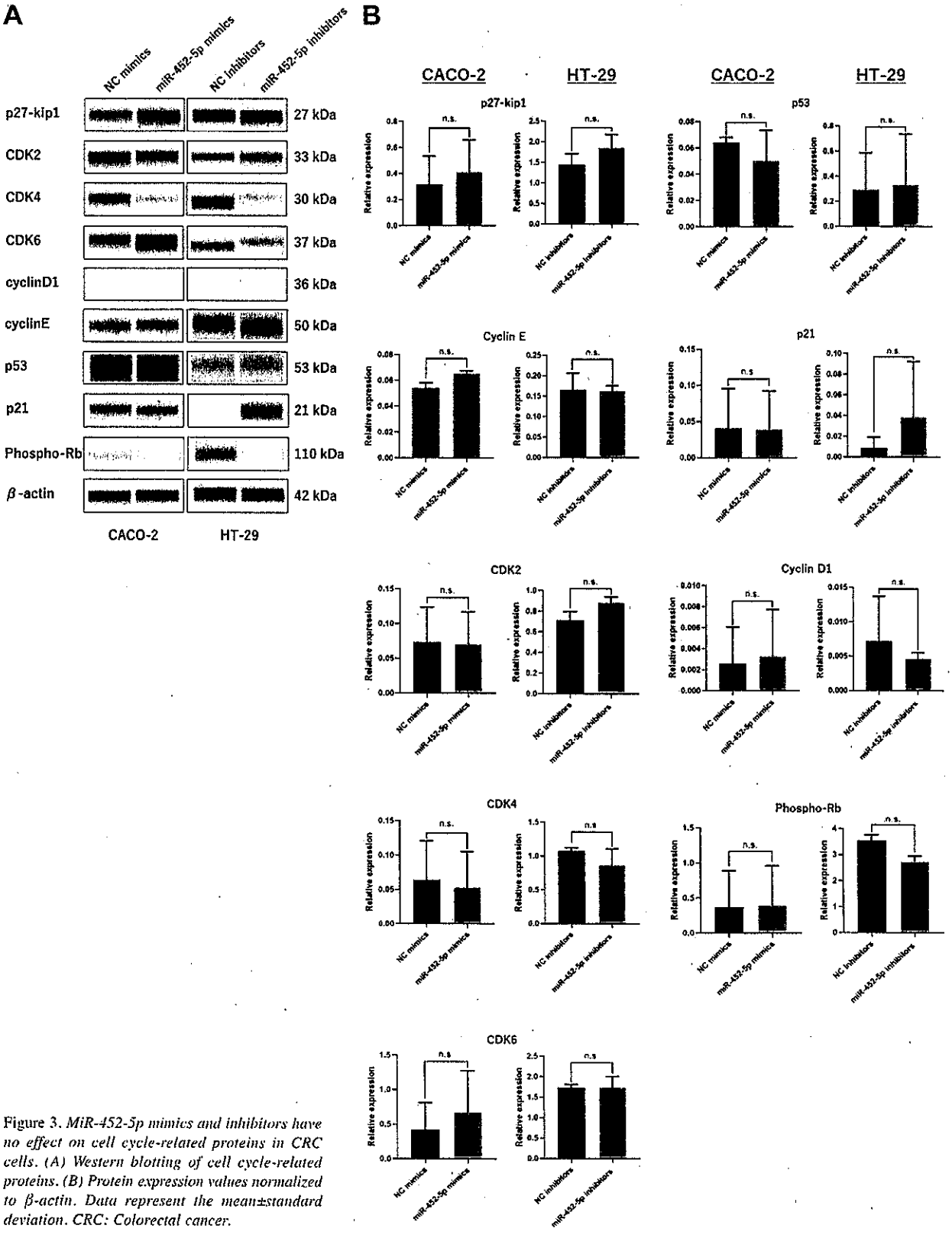

Figure 3. *MiR-452-5p mimics and inhibitors have no effect on cell cycle-related proteins in CRC cells. (A) Western blotting of cell cycle-related proteins. (B) Protein expression values normalized to β-actin. Data represent the mean±standard deviation. CRC: Colorectal cancer.*

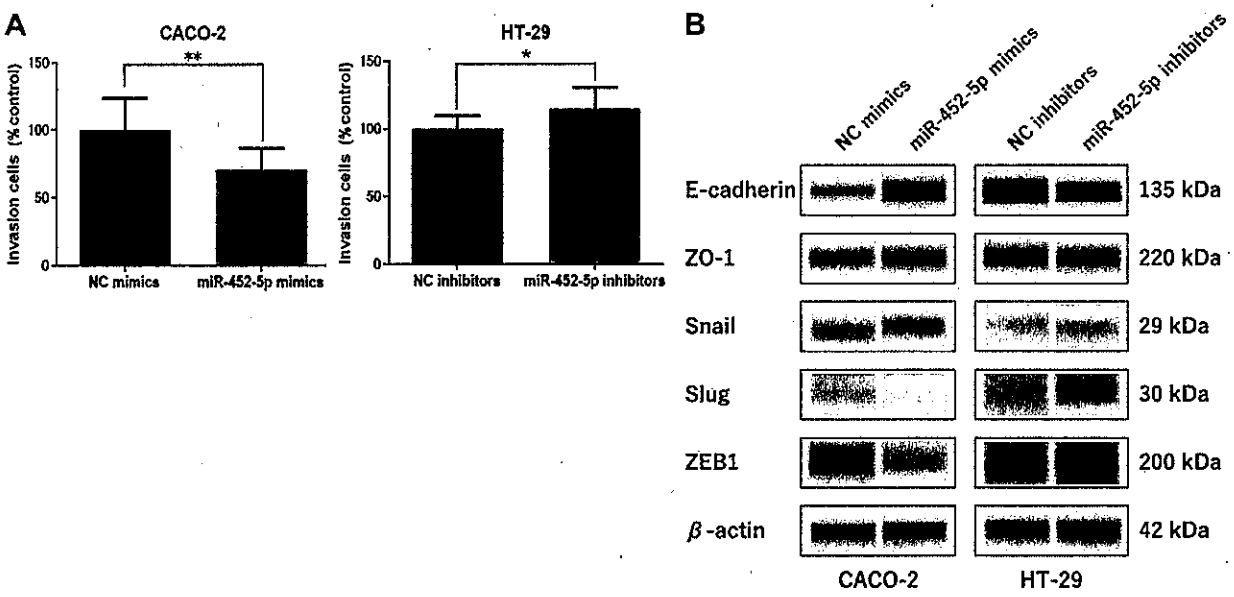

Figure 4. *Continued*

stored at −80°C until use for later analysis. Approval for this study was obtained from the Institutional Review Board of Kagawa University (no. Heisei 22-063) and the study was conducted in accordance with the World Medical Association Declaration of Helsinki Ethical Principles for Medical Research Involving Human Subjects. All patients were fully informed and gave written consent for the use of clinical samples and data.

Microarray analysis of miRNAs. A miRNA array analysis was performed as described in our previous study (12). We used the miRNAeasy Mini Kit (Qiagen, Hilden, Germany) to extract total RNA from tissue samples according to the manufacturer's instructions. The miRCURYHy3/Hy5 Power Labeling Kit and human miRNA Oligo Chips (v. 21.0; Toray Industries, Tokyo, Japan) were used for the miRNA expression analysis. Raw data were analyzed with the GeneSpringGX 10.0 software (Agilent Technologies, Tokyo, Japan). Quantile normalization was performed on the huge amount of raw data, and Mann-Whitney *U*-tests were used to identify miRNAs with different expression levels. Hierarchical clustering was created using the shortest distance method with Pearson's absolute correlation coefficient as the index. Heat maps were created on the basis of relative expression intensity of each miRNA between tumor and non-tumor areas using log2 of the fold change.

Real-time quantitative reverse transcription-polymerase chain reaction. We quantified miR-4633-5p, miR-452-5p, miR-887-5p, miR-769-5p, and miR-572 from total RNA extracted from tissue samples using human TaqMan MicroRNA Assay Kits (Applied Biosystems, Foster City, CA, USA). We purchased all primers and probes from Applied Biosystems and used RNU6B as an internal control. Relative quantification of miRNA was performed by real-time quantitative reverse transcription-polymerase chain reaction (qRT-PCR) using the ViiA7 real-time PCR system (Applied Biosystems). Relative quantification of miRNAs was analyzed by the $2^{-\Delta\Delta CT}$ method (17).

Cell lines and cell cultures. Seven human CRC cell lines (CACO-2, COLO-320, HCT-116, HCT-8, LOVO, CW-2, and HT-29) were purchased. CACO-2, COLO-320, and CW-2 cells were purchased from RIKEN BRC (Tsukuba, Japan). HCT-116 and HCT-8 cells were purchased from the American Type Culture Collection (Manassas, VA, USA). LOVO cells were purchased from the Japanese Collection of Research Bioresources Cell Bank (Osaka, Japan). HT-29 cells were purchased from the Cell Lines Service (Eppelheim, Deutschland). COLO-320, CW-2 and HCT-8 cells were cultured in RPMI-1640 medium (Fujifilm Wako Pure Chemical Corporation, Osaka, Japan). 10% fetal bovine serum [(FBS) Mediatech, Inc., Woodland, CA, USA] was supplemented for COLO-320 and CW-2 cells, and 10% horse serum (Life Technologies Corporation, Grand Island, NY, USA) was supplemented for HCT-8 cells. CACO-2 and HT-29 cells were cultured in MEM medium (Wako). 20% FBS and 1% Non-essential Amino Acids Solution (Nacalai Tesque, Inc., Kyoto, Japan) were supplemented for CACO-2 cells, and 10% FBS was supplemented for HT-29 cells. HCT-116 cells were cultured in McCoy's 5A medium (Life Technologies Corporation) supplemented with 10% FBS, and LOVO cells were cultured in Ham's F-12 medium (Wako) supplemented with 10% FBS. All media were supplemented with 100 mg/ml penicillin/streptomycin (Thermo Fisher Scientific, Waltham, MA, USA) and cultured under humidified conditions of 5% CO_2 and 37°C.

Cell transfection. We obtained miR-452-5p mimics (cat. no. 4464066) and inhibitors (cat. no. 4464084) and negative control miRNA from Thermo Fisher Scientific. CACO-2 and HT-29 cells were seeded in 96-well or six-well plates and cultured for 24 h. The cells were then transfected with appropriately adjusted miRNAs with Lipofectamine RNAiMAX (Life Technologies Corporation)

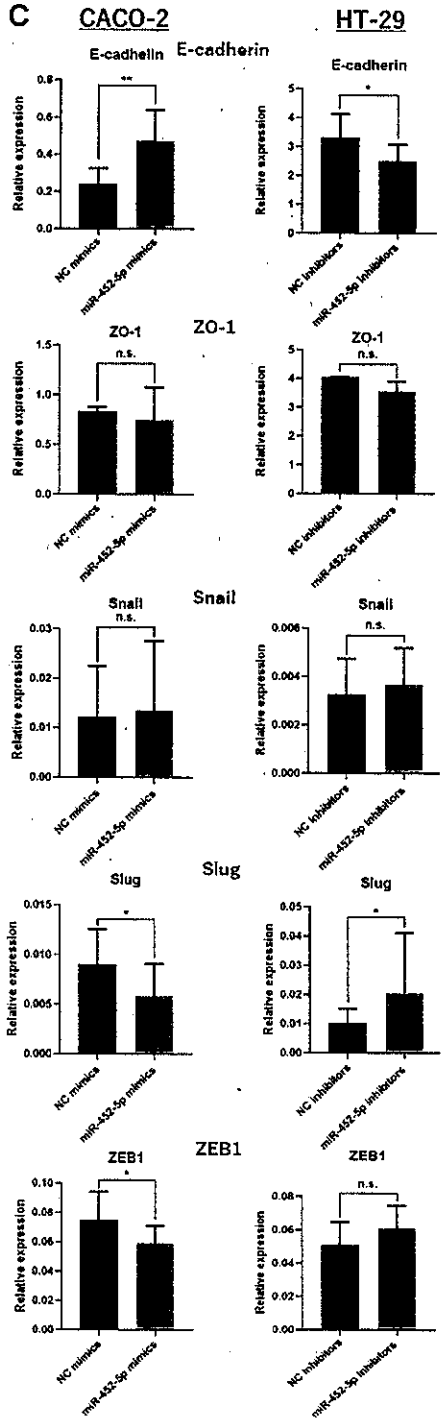

Figure 4. *MiR-452-5p suppresses EMT in CRC cells and negatively affects CRC cell invasion. (A) Transwell invasion assays of CRC cells treated with miR-452-5p mimics or inhibitors compared to control RNAs. (B)Western blotting of EMT-related proteins. (C) Protein expression values normalized to β-actin. Data represent the mean±standard deviation. *p<0.05, **p<0.01 vs. the control group. EMT: Epithelial-mesenchymal transition; CRC: colorectal cancer.*

following the manufacturer's protocol. CACO-2 cells were treated with mimics or negative controls, and HT-29 cells were treated with inhibitors or negative controls. After 48 h of incubation, cells were collected, washed with ice-cold phosphate-buffered saline, and used for experiments.

Cell proliferation assay. Assays for cell proliferation were performed using the cell counting kit-8 (CCK-8) assay (Dojindo Laboratories, Kumamoto, Japan). Cells were seeded in 96-well plates at a density of 5.0×10^3 cells/well and cultured. After 24 h, each cell was transfected with adjusted miRNA and incubated at 37˚C, at 5% CO_2 for another 48 or 96 h. The medium in each well was then replaced with medium containing CCK-8 reagent, and the plates were incubated for an additional 3 h. The absorbance at 450 nm was measured using a microplate reader (Multiskan FC; Thermo Fisher Scientific, Tokyo, Japan). The experiments were repeated three times.

Cell cycle analysis. We used the Cycle Phase Determination kit (Cayman Chemical Company, Ann Arbor, MI, USA) for a flow cytometric analysis. CACO-2 and HT-29 cells were seeded in six-well plates and cultured for 24 h. Adjusted miRNAs were then transfected in each well and incubated for 48 h. The cells were collected in three wells as a single sample to ensure sufficient cell numbers. Flow cytometry was performed using a Cytomics FC 500 flow cytometer (Beckman Coulter, Indianapolis, IN, USA) and the data was analyzed with Kaluza Analysis software (v2.1; Beckman Coulter). All experiments were performed in triplicate.

Invasion assays. We used the CytoSelect 96-well Cell Invasion Assay Kit (Cell Biolabs, San Diego, CA, USA) according to the manufacturer's instructions to evaluate cell invasion. Briefly, 1.0×10^6/ml serum-free medium cell suspension was prepared, and adjusted miRNAs were mixed into the cell suspension of each cell and incubated for 48 h. The cells that had invaded the bottom of the membrane were stained, and their fluorescence was quantified at 480 nm/520 nm using a spectrophotometer (SH-9000lab; Corona Electric Co., Ibaraki, Japan). The experiments were repeated three times.

Automated western immunoblotting. We used the automated, capillary-based Simple Western system (Abby; ProteinSimple, Santa Clara, CA, USA) to detect and quantify our proteins of interest. CACO-2 and HT-29 cells were seeded in six-well plates and incubated for 24 h. Adjusted miRNA was then transfected in each well and incubated for another 48 h. The cells were washed twice in phosphate-buffered saline and lysed in PRO-PREP complete protease inhibitor mixture (iNtRON Biotechnology, Seongnam, Republic of Korea). The final lysates were adjusted to 1.0 μg/μl or 2.0 μg/μl. Capillary western immunoblotting was performed according to the manufacturer's instructions. Results were analyzed by Compass Simple Western software (version 4.1.0, ProteinSimple). The following primary antibodies were used: E-cadherin (#3195; 1:50 dilution), Snail (#3879; 1:10 dilution), Slug (#9585; 1:10 dilution), TCF8/ZEB1 (#3396; 1:10 dilution), ERK1/2 (#4695; 1:10 dilution), p-ERK1/2 (#4370; 1:20 dilution), p27-kip1 (#3698; 1:10 dilution), p53 (#2524; 1:10 dilution), CDK4 (#12790; 1:10 dilution), Cyclin D1 (#55506; 1:10 dilution), phospho-Rb (#9307; 1:10 dilution), CDK2 (#2546; 1:10 dilution), p21 (#2947; 1:10 dilution), and β-actin (#3700; 1:250 dilution) obtained from Cell Signaling Technology; Cyclin E (cat. no. 51-1459; 1:10 dilution) obtained from BD Biosciences Pharmingen™ (Franklin

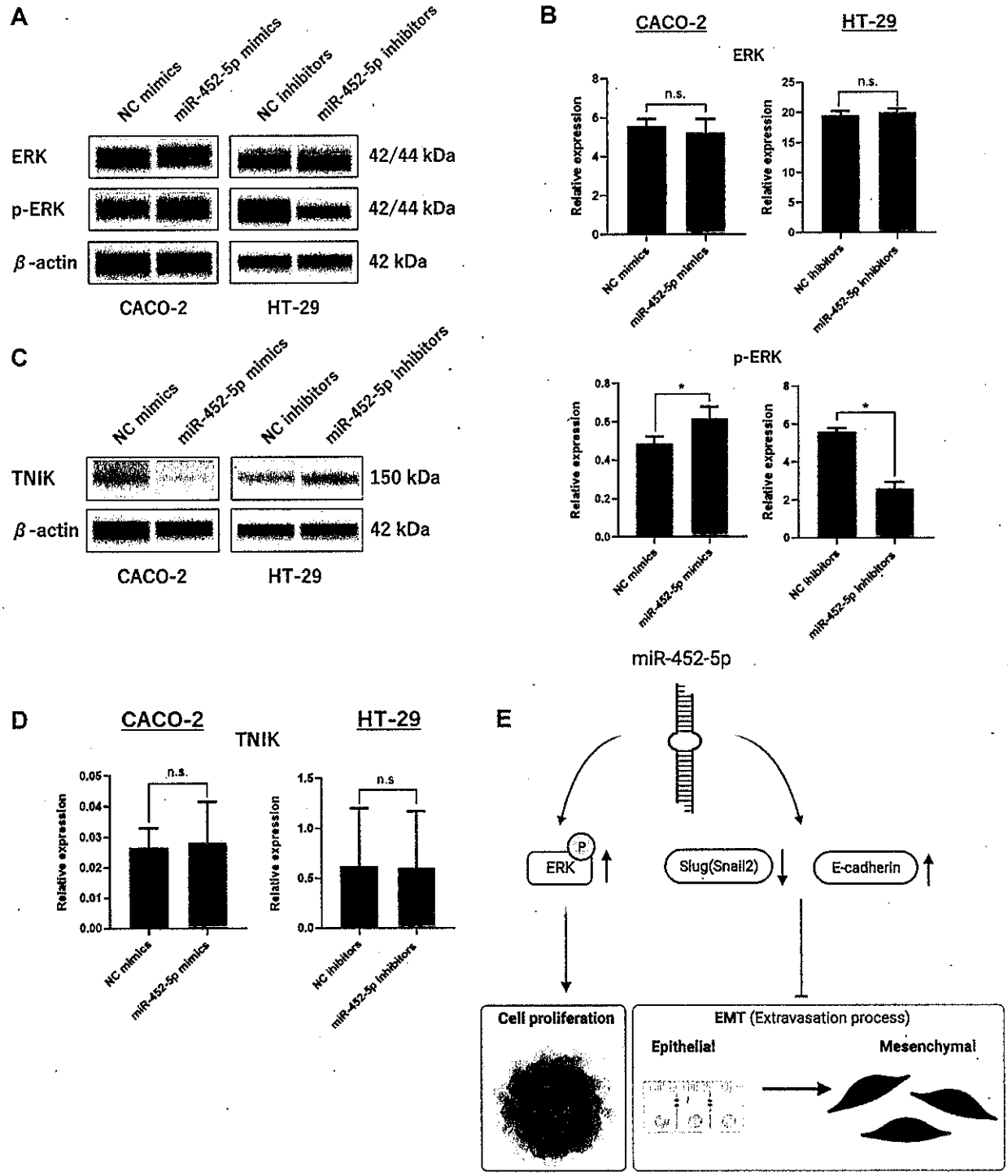

Figure 5. *MiR-452-5p is involved in promoting cell proliferation by activating the ERK pathway and suppressing EMT by suppressing Slug. (A) Western blotting of ERK and p-ERK. (B) Protein expression values normalized to β-actin. (C) Western blotting of TNIK. (D) Protein expression values normalized to β-actin. (E) Hypothetical model for the role of miR-452-5p in CRC. In this model, miR-452-5p promotes phosphorylation of ERK and promotes cell proliferation in CRC cell lines. MiR-452-5p suppresses EMT in CRC cells by repressing Slug and inducing E-cadherin expression (Figure created at biorender.com). Data represent the mean±standard deviation. *p<0.05 vs. the control group. p: Phosphorylated; EMT: epithelial-mesenchymal transition; ERK: extracellular signal-regulated kinase; TNIK: TRAF2 and NCK-interacting protein kinase; CRC: colorectal cancer.*

Lakes, NJ, USA); CDK6 (cat. no. 124821; 1:2,500 dilution) obtained from Abcam (Cambridge, UK); and TNIK (sc-3777215; 1:10 dilution) obtained from Santa Cruz Biotechnology (Dallas, TX, USA). Anti-Rabbit Detection Module (ProteinSimple, DM-001) and Anti-Mouse Detection Module (ProteinSimple, DM-002) were used as secondary antibodies. β-actin was used as a housekeeping control, and the data were normalized by β-actin. All experiments were performed in tenfold.

Statistical analysis. All statistical analyses were performed using the GraphPad Prism software v9.5 (GraphPad Software, San Diego, CA, USA). Statistical significance between the two groups was assessed using the nonparametric Wilcoxon/Mann-Whitney *U*-test. $p<0.05$ was considered statistically significant.

Results

MiR-452-5p is up-regulated in early-stage CRC. Fifteen paired samples of CRC tissue and adjacent normal tissue had sufficient material for miRNA analysis. The patients' and tumors' characteristics are shown in Table I. The pathological diagnosis of ESD lesions was adenoma in four cases, intramucosal carcinoma (M) in two cases, SM1 carcinoma in two cases, and SM2 carcinoma in seven cases. We first analyzed the differences in miRNA expression between early-stage CRC tissue and adjacent normal tissue in each sample by microarray analysis. Hierarchical clustering analysis showed that the 2 tissue groups clearly formed different clusters, and 26 of the 2555 miRNAs showed different expression (Figure 1A). Among these, a total of 11 miRNAs exhibited significant upregulation, while 15 miRNAs exhibited significant downregulation in early-stage CRC tissue compared with adjacent normal tissue (Table II). Next, qRT-PCR was performed on 15 CRC tissue samples and matched adjacent normal tissue samples to validate the miRNAs that were significantly different in the microarray analysis. The expression of miR-452-5p was up-regulated in early-stage CRC tissues approximately 2.3-fold compared with adjacent normal tissue ($p<0.05$). However, there was no significant difference in the expression levels of other miRNAs (miR-4633-5p, miR-452-5p, miR-887-5p, miR-769-5p, and miR-572) (Figure 1B).

MiR-452-5p promotes CRC cell proliferation in vitro. To further investigate the biological function of miR-452-5p in CRC, we compared miR-452-5p expression levels by qRT-PCR in seven human CRC cells (CACO-2, COLO-320, HCT-116, HCT-8, LOVO, CW-2, and HT-29). We found that miR-452-5p expression was significantly lower in CACO-2 cells and significantly higher in HT-29 cells than in the seven CRC cell types (Figure 2A).

The effectiveness of transfection of miR-452-5p mimics or inhibitors in CACO-2 and HT-29 cells was then assessed by the CCK-8 assay. Cell proliferation was significantly promoted in CACO-2 cells transfected with the miR-452-5p mimic and significantly suppressed in HT-29 cells transfected with the miR-452-5p inhibitor ($p<0.05$, Figure 2B). The CCK-8 assay showed that miR-452-5p mimic transfection in CACO-2 cells accelerated cell proliferation from 48 h, while miR-452-5p inhibitor transfection in HT29 cells delayed cell proliferation from 48 h ($p<0.05$, Figure 2B). To further confirm the association between the cell proliferation effect and the cell cycle, cell cycle alterations were assayed by flow cytometry (Figure 2C). We found that miR-452-5p promoted cell cycle transformation in CACO-2 cells (Figure 2C). However, in HT29 cells, miR-452-5p inhibitors increased the percentage of G0/G1 cycles, although this was not statistically significant.

Automated western blotting was also performed to detect the amount of cell cycle-related proteins (Figure 3A). We found that miR-452-5p mimics and inhibitors had no effect on cell cycle-related proteins in CACO-2 and HT-29 cells (Figure 3B). Taken together, these findings suggest that miR-452-5p promotes CRC proliferation *in vitro*, indicating that miR-452-5p contributes to CRC proliferation.

MiR-452-5p is involved in upregulation of E-cadherin expression via suppression of Slug and negatively affects CRC cell invasion. CACO-2 and HT-29 cells were then used to assess the effects of miR-452-5p on cell invasion and EMT induction. The invasiveness of CACO-2 cells was suppressed after transfection of miR-452-5p mimics, while transfection of HT-29 cells with miR-452-5p inhibitors had the opposite effect (Figure 4A). Furthermore, western blotting showed that transfection of miR-452-5p mimics suppressed Slug expression and enhanced E-cadherin expression in CACO-2 cells (Figure 4B, C). The opposite effect was detected after transfecting miR-452-5p inhibitors in HT-29 cells (Figure 4C). These results suggest that miR-452-5p suppresses EMT in CRC cells by repressing Slug and inducing E-cadherin expression.

MiR-452-5p is involved in promoting cell proliferation by activating the extracellular signal-regulated kinase (ERK) pathway and suppressing EMT by suppressing Slug. To confirm that miR-452-5p is involved in cell proliferation, we examined changes in extracellular signal-regulated kinase (ERK), which is one of the proteins involved in the cell proliferation pathway. We found that miR-452-5p promoted phosphorylation of ERK in CACO-2 cells, but the opposite effect was detected when an miR-452-5p inhibitor was transfected into HT-29 cells (Figure 5A and B).

To further investigate the mechanism of miR-452-5p and EMT in CRCs, target prediction of miR-452-5p was performed using the miRDB and TargetScan databases. Among the candidate genes, miR-452-5p may suppress EMT by inactivating TRAF2 and NCK-interacting kinase (TNIK) and blocking Wnt/β signaling (21). The mimics

and inhibitors of miR-452-5p had no effect on TNIK expression in CACO-2 and HT-29 cells (Figure 5C and D). These results suggest that miR-452-5p is involved in promoting cell proliferation by activating the ERK pathway and suppressing EMT by suppressing Slug (Figure 5E).

Discussion

In the present study, we found that miR-452-5p was up-regulated in CRC cell lines and tissue of early-stage CRC. Previous reports have shown that miR-452-5p is overexpressed in CRC tissue compared to the adjacent normal tissue (9, 10, 16), but all these reports were limited to advanced cancers. Furthermore, miR-452-5p promotes cell proliferation through activation of the ERK/MAPK signaling pathway but tends to exert a positive effect on the G1 to S transition of the cell cycle as a mechanism. However, miR-452-5p inhibits cell invasion through suppression of Slug expression and the up-regulation of E-cadherin expression. Studies have shown that miR-452-5p targets multiple genes and has a key role in cancer development and pathogenesis through various mechanisms (14). Previous studies have shown that miR-452-5p plays a dual role as a potential tumor suppressor and candidate cancer gene in several human cancers (15-20). Additionally, miR-452-5p may play a dual role in CRC in promoting cell proliferation and as a suppressor of invasion.

To elucidate the functional role of differentially expressed miRNAs in CRC, we analyzed the effects of overexpression and inhibition of miR-452-5p on CRC cell growth and invasion *in vitro*. Previous reports have shown that miR-452-5p promotes tumorigenesis in hepatocellular carcinoma and CRC and confers resistance to docetaxel in breast cancer cells. (15, 16). However, miR-452-5p also inhibits the progression of non-small cell lung cancer and prostate cancer (17, 18). In previous studies, miR-452-5p promoted tumor cell growth in CRC (9, 16), and our results are consistent with these studies. Additionally, miR-452-5p promotes cell proliferation and affects the cell cycle through activation of the ERK signaling pathway in CRC.

Few reports have focused on the relationship between miR-452-5p and cancer cell invasion. Migration and invasion of hepatocellular carcinoma are promoted by miR-452-5p *via* COLEC10 (19). Additionally, sunitinib –a multi-target receptor tyrosine kinase inhibitor– suppresses renal cell carcinoma invasion and migration by downregulating miR-452-5p expression (20). However, miR-452-5p inhibited colon cancer cell invasion in our study. Additionally, miR-452-5p suppressed EMT in CRC cells by repressing Slug and inducing E-cadherin expression. Previous studies have shown that coexistence of high Slug expression and low E-cadherin expression in patients with CRC is associated with a poor prognosis, whereas patients with low Slug expression and high E-cadherin expression have a good prognosis (21). Slug overexpression promotes EMT and leads to invasion and metastasis in CRC, suggesting that miR452-5p inhibits EMT by suppressing Slug expression. Furthermore, Slug and TNIK are predicted by target scan to be target genes of mir-452-5p. TNIK is a promising therapeutic target for CRC because of its essential roles in regulating the Wnt/β-catenin signaling pathway (22). Therefore, miR-452-5p may regulate EMT by directly targeting Slug. However, miR-452 was previously reported to promote cell invasion by directly targeting GSK3β in CRC (16), which contradicts our results. This inconsistent function of miR-452-5p may be due to differences in cell lines and their tissue specificity. The expression levels of GSK3β and E-cadherin have been implicated in migration, chemotaxis, metastasis, and clinical prognosis in colorectal cancer cell lines and tissues (23), and further studies on the relationship between these factors are needed.

In conclusion, this study revealed miRNA expression characteristic of early-stage CRC. The miRNA miR-452-5p promotes cell proliferation through activation of the ERK pathway, while inhibiting cell invasion through suppressing Slug expression and up-regulating E-cadherin expression. Among the miRNAs, miR-452-5p is overexpressed in early-stage CRC and has two aspects of promoting cell proliferation and inhibiting invasion in CRC cells.

Funding

This work was supported by the Japan Society for the Promotion of Science (JSPS) KAKENHI (grant number: 21K15646) and by the Alumni Association of the Faculty of Medicine, Kagawa University (No. R3-2).

Conflicts of Interest

The Authors declare no conflicts of interest.

Authors' Contributions

YK, TC, TMatsui, and TMasaki designed the experiments. SH, KF, JT, AM, HK, MO, and HI conducted the experiments, data analysis, and final drafting and writing of the manuscript. SF was involved in the research design and contributed to drafting of the manuscript. All Authors have read and agreed to the published version of the manuscript.

Acknowledgements

We thank Kayo Hirose, Megumi Okamura, Mari Yamada, Fuyuko Kokado, and Keiko Fujikawa for their skillful technical assistance. We thank Edanz (https://jp.edanz.com/ac) for editing a draft of this manuscript.

References

1 Sung H, Ferlay J, Siegel RL, Laversanne M, Soerjomataram I, Jemal A, Bray F: Global cancer statistics 2020: GLOBOCAN estimates of incidence and mortality worldwide for 36 cancers in 185 countries. CA Cancer J Clin 71(3): 209-249, 2021. DOI: 10.3322/caac.21660

2 Yeung KT, Yang J: Epithelial-mesenchymal transition in tumor metastasis. Mol Oncol 11(1): 28-39, 2017. DOI: 10.1002/1878-0261.12017

3 Thiery JP, Acloque H, Huang RY, Nieto MA: Epithelial-mesenchymal transitions in development and disease. Cells 139(5): 871-890, 2009. DOI: 10.1016/j.cell.2009.11.007

4 Loh C, Chai J, Tang T, Wong W, Sethi G, Shanmugam M, Chong P, Looi C: The E-cadherin and N-cadherin switch in epithelial-to-mesenchymal transition: Signaling, therapeutic implications, and challenges. Cells 8(10): 1118, 2019. DOI: 10.3390/cells8101118

5 Mendonsa AM, Na TY, Gumbiner BM: E-cadherin in contact inhibition and cancer. Oncogene 37(35): 4769-4780, 2018. DOI: 10.1038/s41388-018-0304-2

6 Wang Y, Shi J, Chai K, Ying X, Zhou BP: The role of snail in EMT and tumorigenesis. Curr Cancer Drug Targets 13(9): 963-972, 2013. DOI: 10.2174/15680096113136660102

7 Hu Y, Dai M, Zheng Y, Wu J, Yu B, Zhang H, Kong W, Wu H, Yu X: Epigenetic suppression of E-cadherin expression by Snail2 during the metastasis of colorectal cancer. Clin Epigenetics 10(1): 154, 2018. DOI: 10.1186/s13148-018-0592-y

8 O'brien J, Hayder H, Zayed Y, Peng C: Overview of microRNA biogenesis, mechanisms of actions, and circulation. Front Endocrinol (Lausanne) 9: 402, 2018. DOI: 10.3389/fendo.2018.00402

9 Lin X, Han L, Gu C, Lai Y, Lai Q, Li Q, He C, Meng Y, Pan L, Liu S, Li A: MiR-452-5p promotes colorectal cancer progression by regulating an ERK/MAPK positive feedback loop. Aging (Albany NY) 13(5): 7608-7626, 2021. DOI: 10.18632/aging.202657

10 Yan J, Wei R, Li H, Dou Y, Wang J: miR-452-5p and miR-215-5p expression levels in colorectal cancer tissues and their relationship with clinicopathological features. Oncol Lett 20(3): 2955-2961, 2020. DOI: 10.3892/ol.2020.11845

11 Dixon MF: Gastrointestinal epithelial neoplasia: Vienna revisited. Gut 51(1): 130-131, 2002. DOI: 10.1136/gut.51.1.130

12 Fujihara S, Kobara H, Nishiyama N, Hirose K, Iwama H, Masaki T: MicroRNA expression profiles in superficial esophageal squamous cell carcinoma before endoscopic submucosal dissection: A pilot study. Int J Mol Sci 22(9): 4789, 2021. DOI: 10.3390/ijms22094789

13 Livak KJ, Schmittgen TD: Analysis of relative gene expression data using real-time quantitative PCR and the $2^{-\Delta\Delta CT}$ method. Methods 25(4): 402-408, 2001. DOI: 10.1006/meth.2001.1262

14 Kolligs FT: Diagnostics and epidemiology of colorectal cancer. Visc Med 32(3): 158-164, 2016. DOI: 10.1159/000446488

15 Zheng Q, Sheng Q, Jiang C, Shu J, Chen J, Nie Z, Lv Z, Zhang Y: MicroRNA-452 promotes tumorigenesis in hepatocellular carcinoma by targeting cyclin-dependent kinase inhibitor 1B. Mol Cell Biochem 389(1-2): 187-195, 2014. DOI: 10.1007/s11010-013-1940-z

16 Li T, Jian X, He H, Lai Q, Li X, Deng D, Liu T, Zhu J, Jiao H, Ye Y, Wang S, Yang M, Zheng L, Zhou W, Ding Y: MiR-452 promotes an aggressive colorectal cancer phenotype by regulating a Wnt/β-catenin positive feedback loop. J Exp Clin Cancer Res 37(1): 238, 2018. DOI: 10.1186/s13046-018-0879-z

17 Zhang Y, Han L, Pang J, Wang Y, Feng F, Jiang Q: Expression of microRNA-452 *via* adenoviral vector inhibits non-small cell lung cancer cells proliferation and metastasis. Tumour Biol 37(6): 8259-8270, 2016. DOI: 10.1007/s13277-015-4725-z

18 Goto Y, Kojima S, Kurozumi A, Kato M, Okato A, Matsushita R, Ichikawa T, Seki N: Regulation of E3 ubiquitin ligase-1 (WWP1) by microRNA-452 inhibits cancer cell migration and invasion in prostate cancer. Br J Cancer 114(10): 1135-1144, 2016. DOI: 10.1038/bjc.2016.95

19 Zheng J, Cheng D, Wu D, Wang L, Qu F, Wu X, Cheng L, Wei Y, Liu X: MiR-452-5p mediates the proliferation, migration and invasion of hepatocellular carcinoma cells *via* targeting COLEC10. Per Med 18(2): 97-106, 2021. DOI: 10.2217/pme-2020-0027

20 Zhai W, Li S, Zhang J, Chen Y, Ma J, Kong W, Gong D, Zheng J, Xue W, Xu Y: Sunitinib-suppressed miR-452-5p facilitates renal cancer cell invasion and metastasis through modulating SMAD4/SMAD7 signals. Mol Cancer 17(1): 157, 2018. DOI: 10.1186/s12943-018-0906-x

21 Shioiri M, Shida T, Koda K, Oda K, Seike K, Nishimura M, Takano S, Miyazaki M: Slug expression is an independent prognostic parameter for poor survival in colorectal carcinoma patients. Br J Cancer 94(12): 1816-1822, 2006. DOI: 10.1038/sj.bjc.6603193

22 Kukimoto-Niino M, Shirouzu M, Yamada T: Structural insight into TNIK inhibition. Int J Mol Sci 23(21): 13010, 2022. DOI: 10.3390/ijms232113010

23 Park Y, Cho S, Park S, Oh H, Myung E, Im C, Son S, Kim S, Cho S, Chung M, Hong J, Kim K, Myung D, Lee W, Park D, Joo Y: Engulfment and cell motility 1 (ELMO1) regulates tumor cell behavior and predicts prognosis in colorectal cancer. Anticancer Res 42(11): 5343-5355, 2022. DOI: 10.21873/anticanres.16058

Received May 29, 2023
Revised July 3, 2023
Accepted July 17, 2023